Kim, *ibid.* 23, 1375 (1970).
[8]C. Bloch and C. De Dominicis, Nucl. Phys. 7, 459 (1963).
[9]C. De Dominicis and G. Toulouse, Physica (to be published).
[10]H. Suhl, Phys. Rev. 138, 515 (1965).
[11]W. Brenig and W. Götze, Z. Physik 217, 188 (1968).
[12]J. R. Schrieffer and P. A. Wolff, Phys. Rev. 149, 491 (1966).
[13]G. Toulouse and B. Coqblin, Solid State Commun. 7, 853 (1969).
[14]P. W. Anderson and G. Yuval, Phys. Rev. Letters 23, 89 (1969); G. Yuval and P. W. Anderson, Phys. Rev. B 1, 1522 (1970); P. W. Anderson, G. Yuval, and D. R. Hamann (report of work prior to publication).
[15]P. Nozières and C. DeDominicis, Phys. Rev. 178, 1097 (1969).
[16]G. Toulouse, Compt. Rend. 268, 1200 (1969); 268, 1257 (1969).
[17]R. L. Stratonovitch, Dokl. Akad. Nauk. SSSR 115, 1097 (1957) [Soviet Phys. Doklady 2, 416 (1958)].
[18]D. J. Scalapino, Phys. Rev. Letters 16, 937 (1966).
[19]A. A. Abrikosov, Physics 2, 5 (1965).
[20]P. Nozières, J. Gavoret, and B. Roulet, Phys. Rev. 178 1084 (1969).

PHYSICAL REVIEW B VOLUME 2, NUMBER 2 15 JULY 1970

# Long-Range Order in $\beta$ Brass

J. C. Norvell* and J. Als-Nielsen†
*Physics Department, Research Establishment Risö, The Danish Atomic Energy Commission, Roskilde, Denmark*
(Received 18 February 1970)

The long-range order parameter $M$ of $\beta$ brass has been determined from measurements of the intensity of superlattice reflections of Bragg-scattered neutrons. Over the whole temperature range $T = 300$ °K to $T = T_c = 736$ °K, the data are in remarkable agreement with the prediction for the compressible Ising bcc lattice with only nearest-neighbor interactions.

## I. INTRODUCTION

The alloy $\beta$ brass is composed of approximately equal parts of Cu and Zn. At room temperature the cube corners of the bcc lattice are predominantly occupied by one type of atom – say Cu atoms – and the centers by Zn atoms. As the temperature is raised, the occupation of lattice sites becomes more and more random, until at the critical temperature $T_c$ the average occupation of a lattice site is entirely random. Even above $T_c$, however, the occupation of lattice sites is correlated in the sense that if a certain site is occupied by a Cu atom, there will be an excess probability over randomness that the nearest-neighbor sites are occupied by Zn atoms and so on. The occupation of lattice sites can be studied by a diffraction experiment and in this paper we describe a measurement of the average occupation of a lattice site below $T_c$. This average occupation of a lattice site is a measure of the long-range order and corresponds to the magnetization in an Ising magnet. In an earlier study, Chipman and Warren[1] examined the long-range order in $\beta$ brass by x-ray diffraction.

It has been emphasized previously that the order-disorder transition in $\beta$ brass provides an exceptional possibility for an accurate comparison between experiment and a relevant theory for phase transitions. This is because the configurational energy in the alloy is formally given by the Ising-magnet Hamiltonian, a model which is sufficiently simple to allow detailed theoretical calculations. Indeed, previous neutron scattering experiments have verified the theoretical predictions for the correlation range and the temperature dependence of the magnetization and of the susceptibility.[2-4] As we shall see, the results of the present experiment on the average occupation of a lattice site are also in very good agreement with theory.

The Bragg-scattering cross section $(d\sigma/d\Omega)_B$ for a superlattice reflection from a rigid lattice is

$$\left(\frac{d\sigma}{d\Omega}\right)_B = \tfrac{1}{4}N^2 (f_{\mathrm{Cu}} - f_{\mathrm{Zn}})^2 M^2 \delta(\vec{K} - \vec{\tau}) \quad . \qquad (1)$$

Here $N$ is the number of atoms in the single-crystal sample, and $f_{\mathrm{Cu}}$ and $f_{\mathrm{Zn}}$ the scattering amplitudes of Cu and Zn atoms, respectively. The scattering vector $\vec{K}$ is the difference between the incident and scattered neutron wave vectors, $\vec{\tau}$ is a reciprocal superlattice vector, i.e., a vector in reciprocal space with an odd sum of indices, and $M$ gives the average occupation of a lattice site. Let $S_i$ be defined as $+1$ if the lattice site at position $\vec{r}_i$ is occupied by a Cu atom and $-1$ if it is occupied by a Zn atom, then $M = \langle \sum_i S_i e^{i\vec{\tau}\cdot\vec{r}_i} \rangle$. The temperature dependence of $M$ near $T_c$ can be expressed by the power law

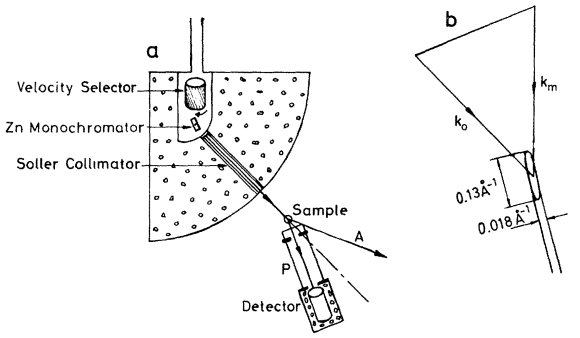


FIG. 1. (a) Neutron diffractometer. The sample may be oriented to Bragg-scatter neutrons in direction $P$ or $A$ corresponding to "parallel" and "antiparallel" reflections, respectively. (b) Scattering diagram corresponding to neutrons scattered from the monochromator. The distribution function is indicated by its contour for half-peak intensity.

$$M \simeq Dt^{\beta}, \tag{2}$$

where $t$ is the reduced temperature $1 - T/T_c$.

For the rigid bcc lattice the predictions of the Ising model are $0.303<\beta<0.318$ and $D = 1.506$[5,6]. However, the present experiments are carried out at constant pressure, not constant volume, so the effect of the lattice expansion with increasing temperature must be considered. Essam and Baker have calculated the appropriate correction[7] for $\beta$ brass using Domb's model[8] and empirical data for the lattice expansion,[9] the compressibility,[10] and the variation of $T_c$ with pressure.[10] Near $T_c$ a power law is still a good approximation, e.g., in the temperature region $0.003 < t < .03$ Essam and Baker find the effective value of $\beta = 0.293$ and $D = 1.498$.

In principle, the determination of $M(T)$ is very simple. By definition, $M(0)$ equals 1, so according to Eq. (1), $M^2(T)$ is equal to the ratio of Bragg-scattering intensities at finite temperature $T$ and $T = 0$, respectively. It is, however, then presumed that the crystal is similarly irradiated by the neutron beam at all temperatures, i.e., that extinction can be neglected. Furthermore, Eq. (1) neglects the lattice vibrations which must be accounted for by the usual temperature-dependent Debye-Waller factor. In order to decrease extinction one can either use a small crystal or use a superlattice Bragg reflection of low reflectivity, i.e., with large Miller indices. In the latter case, however, the corrections of the Debye-Waller factor become large and the results, thus, correspondingly uncertain, so in practice it is necessary to use a sufficiently small crystal if the extinction corrections are to be made accurately.

## II. APPARATUS AND MEASUREMENTS

A monochromatic beam of neutrons with wave vector 4.94 Å$^{-1}$ was extracted from the reactor beam by means of Bragg reflection from a large Zn single crystal in the (0 0 2) reflection. Higher-order neutrons were effectively removed from the reactor beam by means of a mechanical velocity selector. The collimation of the reactor beam was rather wide (~0.4°), the mosaic spread of the Zn crystal was about 0.3° full width at half-maximum (FWHM) and the collimation of the monochromatic beam was 0.26° (FWHM). This implies a resolution of the monochromatic beam as indicated in Fig. 1(b), where the ellipse around $\vec{k}_0$ indicates the contour for half-peak intensity. The collimation of the scattered beam was determined by a 2×2.5-cm hole, 12 cm from the sample, and by a detector window of 5×6 cm, 65 cm from the sample.

The sample was a single crystal of $\beta$ brass (48-at. % Zn) spark cut from a large single crystal as a cylinder 5 mm in diameter and 6 mm in height with the axis along ⟨0 1 1⟩. By turning the crystal around its axis, the $(h\,0\,0)$ reflections could successively be brought into position to Bragg scatter the incident beam, and there were, thus, no geometrical corrections in comparing the intensities for these reflections. In order to avoid Zn evaporation at higher temperatures, the crystal was encapsulated in a thin stainless-steel container.

The temperature was determined by a thermocouple mounted on the outer side of the stainless-steel container. The thermocouple voltage corresponding to the critical temperature ($T_c = 736.0$ °K for our sample) was determined by the pronounced peak at $T_c$ of the critical scattering at $|\vec{K} - \vec{\tau}| = 0.02$ Å$^{-1}$.[4] The estimated uncertainty in $T_c - T$ was about 0.1 °K.

The temperature dependence of the two superlattice reflections (100) and (300) was measured. The angular settings of the Bragg peak change as a function of temperature due to thermal expansion of the crystal. However, the change in scattering angle was found to be negligible because the collimation between the sample and the detector was very wide. A rocking curve was measured at each temperature. The width of the peak was found to be independent of temperature, so the peak intensity was proportional to the integrated intensity although the proportionality factor was of course different for the (100) and the (300) reflection. The peak intensities for the two superlattice reflections are listed in Table I. The corrections described in Sec. III are substantially different for these two reflections and the agreement between the corrected data supports the reliability of the final results.

## III. CORRECTIONS

### A. Extinction

In a scan where the crystal is rotated around a vertical axis, the integrated intensity $I_{hkl}$ of a Bragg reflection with Miller indices $(hkl)$ is given by

$$I_{hkl} \sim |F_{hkl}|^2 / \sin 2\theta_{hkl} \quad . \tag{3}$$

Here $F_{hkl}$ is the usual geometrical structure factor, including the Debye-Waller factor, and $\theta_{hkl}$ is the Bragg angle of the reflection. In the derivation of Eq. (3) it is assumed that the acceptance angle of the counter is wide, and, also, that extinction can be neglected. The first assumption can be checked in practice by comparing the integrated intensities for "parallel" and "antiparallel" neutron paths (rays $P$ and $A$, respectively, in Fig. 1) from the same reflection. Agreement to better than 3% was obtained for all five reflections investigated. The second assumption can be checked by comparing integrated intensities of different Bragg reflections, or alternatively the correction for extinction can be determined experimentally by this comparison. We empirically determined the extinction coefficient $E_s$ (defined as the ratio be-

TABLE I. Intensities and corrections for the (100) and (300) superlattice reflections.

| | Reduced temperature $t=\frac{T_c-T}{T_c}$ | Intensity (counts per 3 min) (constant background subtracted) $I$ | Critical scattering background $B_{c.s.}$ | Extinction correction $E_s$ | $I'=\left(\frac{I-B_{c.s.}}{E_s}\right)$ | Lattice vibration correction $e^{-B(t)h^2}$ | Normalized order parameter $M=\left[\frac{I'(t)}{I'(0)e^{-B(t)h^2}}\right]^{1/2}$ | Error (in %) |
|---|---|---|---|---|---|---|---|---|
| (001) Reflection | 0.4925 ± 0.0014 | 38 001 ± 140 | | 0.746 | 50 921 ± 188 | 0.941 | 0.983 | 0.20 |
| | 0.4161 ± 0.0010 | 36 742 ± 137 | | 0.750 | 48 940 ± 177 | 0.932 | 0.960 | 0.20 |
| | 0.3479 ± 0.0012 | 36 168 ± 135 | | 0.758 | 47 705 ± 178 | 0.921 | 0.954 | 0.21 |
| | 0.2914 ± 0.0009 | 34 142 ± 132 | | 0.769 | 44 384 ± 172 | 0.910 | 0.924 | 0.22 |
| | 0.2327 ± 0.0007 | 32 171 ± 129 | | 0.785 | 40 985 ± 165 | 0.896 | 0.896 | 0.22 |
| | 0.1759 ± 0.0008 | 29 194 ± 122 | | 0.804 | 36 317 ± 152 | 0.881 | 0.851 | 0.25 |
| | 0.1532 ± 0.0007 | 27 702 ± 120 | | 0.816 | 33 962 ± 147 | 0.874 | 0.826 | 0.26 |
| | 0.1210 ± 0.0007 | 25 497 ± 115 | | 0.833 | 30 621 ± 138 | 0.866 | 0.788 | 0.27 |
| | 0.0998 ± 0.0006 | 21 458 ± 105 | | 0.847 | 25 341 ± 124 | 0.857 | 0.722 | 0.31 |
| | 0.0664 ± 0.0006 | 19 123 ± 99 | | 0.873 | 21 914 ± 113 | 0.844 | 0.675 | 0.38 |
| | 0.0581 ± 0.0009 | 18 162 ± 97 | | 0.880 | 20 632 ± 110 | 0.841 | 0.656 | 0.57 |
| | 0.0438 ± 0.0010 | 16 045 ± 91 | | 0.895 | 17 922 ± 101 | 0.834 | 0.614 | 0.78 |
| | 0.0335 ± 0.0008 | 13 294 ± 83 | | 0.901 | 14 623 ± 91 | 0.830 | 0.555 | 0.81 |
| | 0.0259 ± 0.0005 | 11 747 ± 78 | | 0.919 | 12 780 ± 85 | 0.828 | 0.520 | 0.68 |
| | 0.0205 ± 0.0010 | 10 087 ± 73 | 29 | 0.934 | 10 803 ± 78 | 0.824 | 0.480 | 1.56 |
| | 0.0101 ± 0.0008 | 6 928 ± 61 | 61 | 0.954 | 7 260 ± 64 | 0.819 | 0.395 | 2.49 |
| | 0.0051 ± 0.0004 | 4 453 ± 49 | 103 | 0.973 | 4 470 ± 50 | 0.817 | 0.310 | 2.46 |
| | 0.0035 ± 0.0003 | 3 378 ± 43 | 135 | 0.978 | 3 455 ± 44 | 0.814 | 0.273 | 2.83 |
| (003) Reflection | 0.6091 ± 0.0009 | 5 143 ± 24 | | 0.911 | 5 645 ± 26 | 0.644 | 1.001 | 0.23 |
| | 0.5271 ± 0.0006 | 4 621 ± 22 | | 0.912 | 5 064 ± 24 | 0.594 | 0.990 | 0.23 |
| | 0.4502 ± 0.0008 | 4 223 ± 21 | | 0.914 | 4 619 ± 23 | 0.544 | 0.987 | 0.25 |
| | 0.3274 ± 0.0005 | 3 256 ± 19 | | 0.919 | 3 542 ± 21 | 0.455 | 0.944 | 0.30 |
| | 0.2540 ± 0.0005 | 2 659 ± 18 | | 0.924 | 2 877 ± 20 | 0.394 | 0.915 | 0.35 |
| | 0.1970 ± 0.0005 | 2 118 ± 16 | | 0.929 | 2 278 ± 17 | 0.345 | 0.870 | 0.38 |
| | 0.1548 ± 0.0004 | 1 813 ± 15 | | 0.936 | 1 936 ± 16 | 0.307 | 0.850 | 0.42 |
| | 0.1277 ± 0.0004 | 1 460 ± 13 | | 0.941 | 1 551 ± 14 | 0.281 | 0.795 | 0.46 |
| | 0.0995 ± 0.0005 | 1 150 ± 12 | | 0.947 | 1 214 ± 13 | 0.253 | 0.742 | 0.55 |
| | 0.0868 ± 0.0005 | 1 039 ± 12 | | 0.951 | 1 092 ± 13 | 0.241 | 0.721 | 0.62 |
| | 0.0730 ± 0.0005 | 902 ± 11 | | 0.954 | 945 ± 12 | 0.228 | 0.689 | 0.61 |
| | 0.0592 ± 0.0004 | 811 ± 11 | | 0.959 | 845 ± 11 | 0.214 | 0.673 | 0.75 |
| | 0.0459 ± 0.0004 | 642 ± 10 | | 0.964 | 665 ± 10 | 0.202 | 0.613 | 0.81 |
| | 0.0327 ± 0.0006 | 496 ± 9 | | 0.970 | 511 ± 9 | 0.189 | 0.556 | 1.04 |
| | 0.0259 ± 0.0005 | 412 ± 9 | | 0.975 | 422 ± 9 | 0.183 | 0.514 | 1.21 |
| | 0.0197 ± 0.0006 | 327 ± 8 | 5 | 0.981 | 329 ± 8 | 0.178 | 0.460 | 1.54 |
| | 0.0163 ± 0.0006 | 292 ± 8 | 6 | 0.982 | 291 ± 8 | 0.175 | 0.435 | 1.80 |
| | 0.0130 ± 0.0004 | 266 ± 8 | 8 | 0.984 | 262 ± 8 | 0.173 | 0.416 | 1.82 |
| | 0.0099 ± 0.0005 | 233 ± 7 | 9 | 0.987 | 227 ± 7 | 0.169 | 0.392 | 2.20 |
| | 0.0066 ± 0.0003 | 173 ± 7 | 12 | 0.990 | 162 ± 7 | 0.166 | 0.334 | 2.56 |
| | 0.0035 ± 0.0003 | 112 ± 7 | 16 | 0.993 | 96 ± 7 | 0.164 | 0.259 | 4.44 |

tween the observed integrated intensity and the integrated intensity from an extinction-free crystal) for the (100), (200), (300), (400), and (220) reflections at room temperature, where we know that the long-range order parameter is close to unity. At room temperature, we found $E_s = 0.91$ and 0.75 for the (300) and the (100) reflections, respectively. In order to obtain an approximate analytical expression for $E_s$ to be used at higher temperatures for the (100) and the (300) reflections, we compared the room temperature results for $E_s$ to a relevant theoretical model. Hamilton[11] has calculated $E_s$ for a cylindrical crystal assuming the angular distribution of mosaic blocks in the crystal, $W(\Delta)$ is given by $W(\Delta) = 1/(2\sqrt{3}\eta)$ if $|\Delta| < \eta\sqrt{3}$ and $W(\Delta) = 0$ if $|\Delta| > \eta\sqrt{3}$. The results for $E_s$ are given in terms of the quantity

$$x = (\lambda^3 |F_{hkl}|^2 M^2(T)/V_c^2 \sin 2\theta_{hkl})\, r/\eta\sqrt{3} \qquad (4)$$

and Hamilton found that

$$E_s \approx e^{-8x/3\pi}, \qquad (5)$$

provided that $x \lesssim 0.5$.

Here $V_c$ is the unit-cell volume and $r$ is the radius of the crystal. At room temperature, the mosaic width $\eta$ is the only unknown parameter in Eq. (4), and by fitting the data to Eq. (5), we obtained a value of 0.018° for the width of the assumed distribution $2\sqrt{3}\eta$. We attempted, furthermore, to measure $W(\Delta)$ by using a nearly perfect Ge crystal as monochromator and narrow collimation between monochromator and sample. The angular width of the rocking curve was 0.08° FWHM but the shape of the rocking curve indicated that $W(\Delta)$ might be adequately represented by a superposition of a few distributions each having a width of approximately 0.02°.

We emphasize that the important correction for extinction was determined *experimentally* by comparison of the integrated intensities from five reflections at room temperature. The theoretical calculation is only used as a smooth interpolation at higher temperatures using Eqs. (4) and (5) and with iterated values of $M(T)$.

### B. Lattice Vibrations

The thermal vibrations of the lattice imply that the Bragg-scattering cross section for the rigid lattice [Eq. (1)] is diminished by the Debye-Waller factor $\exp[-\langle(\vec{K}\cdot\vec{u})^2\rangle]$, where $u$ is the amplitude of the vibration. We do not need to specify in detail what the average symbol $\langle\ \rangle$ stands for (the result for a monoatomic Debye solid is well known[12]) but we note that the correction is of the form $\exp[-B_1(T)h^2]$ for any $(h00)$ reflection.

Furthermore, the presence of lattice vibrations implies that some of the neutrons detected are not scattered elastically but have rather created or annihilated a phonon in the scattering process. The count rate from such processes is conventionally called the thermal diffuse scattering (TDS) background. We have estimated this correction using the spherical approximation [Willis,[13] Eqs. (7.7) and (7.9)] and we conclude that the correction to $D$ due to TDS is of the order of 1% for the (300) data and an order of magnitude less for the (100) data. Furthermore, when the TDS correction is small it is, also, of the form $\exp[-B_2(T)h^2]$. The temperature-dependent parameter $B(T) = B_1(T) + B_2(T)$ can thus be determined experimentally by comparing the extinction corrected intensities of the (100) and of the (300) reflections at any temperature.[14] These corrections are ginen in Table I.

### C. Other Corrections

The constant background was measured at several points at each temperature and subtracted from the peak-height intensities.

The critical scattering background was estimated from measurements of the resolution function, the critical scattering intensities above $T_c$, and the known ratio of the scattering above and below $T_c$.[4] This background was small except at the points nearest the ordering temperature.

## IV. RESULTS

The measured and corrected intensities are given in Table I. The corrected peak intensities for each reflection were converted to the long-range order parameter $M(T)$ by normalizing to 0.996 at room temperature. The listed relative errors are less than the inverse square root of the tabulated intensities because several points in the rocking curve were used to obtain each peak intensity, and the actual counting time for the (3 0 0) reflection was 2.5 times that for the (1 0 0) reflection.

The long-range order parameter $M$ is plotted in Fig. 2 versus the reduced temperature $t = 1 - T/T_c$. The top part of this figure is a linear plot, whereas, the bottom part is a double logarithmic plot displaying the power law [Eq. (2)] for the data near $T_c$. It is obvious that the two sets of data of the (100) and of the (300) reflections are consistent, although the corrections for extinction and lattice vibrations are quite different for the two reflections as seen from Table I.

Theoretical predictions of $M(T)$ are, also, shown in Fig. 2. The dashed line in the upper part of Fig. 2 represents the magnetization obtained from the mean field approximation with $S = \frac{1}{2}$. The lower full line is the prediction for the rigid, incompressible Ising bcc lattice and was obtained by the Padé approximant method.[5,6] Essam and Baker[7]

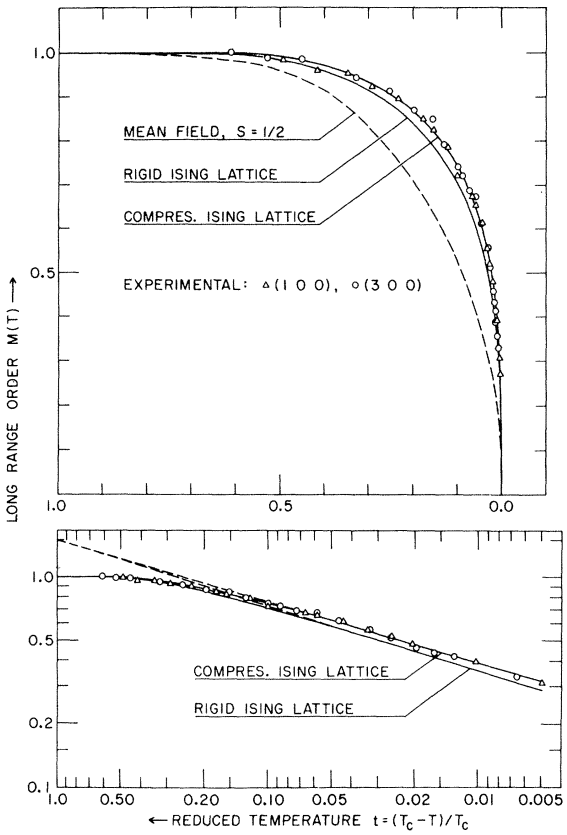


FIG. 2. Long-range order parameter $M(T)$ in $\beta$ brass as determined by the intensity of the (100) and the (300) superlattice Bragg reflections at constant pressure. The data were normalized to 0.996 at room temperature. Also shown are theoretical predictions for $M(T)$ in the mean field approximation (dashed curve), for the Ising magnet at constant volume (lower full line) and for the Ising magnet at constant pressure (upper full line).

have estimated the effect of the compressibility of the lattice using Domb's model.[8] In this model the lattice can only expand *uniformly*, i.e., fluctuations in the nearest-neighbor distance are neglected. The variation of $T_c$ versus volume was obtained from Yoon and Bienenstock's measurements[10] of $T_c$ versus pressure and their estimate of the compressibility at the critical temperature. The variation of the lattice parameter versus temperature was taken from the x-ray data of Owen and Pickup.[9] The results of Essam and Baker are shown as the upper full line in Fig. 2. It is remarkable that the experimental data fit this theoretical curve so well over the whole temperature region, since only nearest-neighbor interactions were assumed in the theory.

TABLE II. Amplitude and exponent of the long-range order for $0.003 < t < 0.03$.

| | $\beta$ | $D$ |
|---|---|---|
| Theoretical value for compressible bcc lattice – Essam and Baker | 0.293 | 1.49 |
| Least-squares fit of data in Fig. 2 varying $D$ and $\beta$ | $0.315 \pm 0.007$ | $1.63 \pm 0.05$ |
| Least-squares fit of data in Fig. 2 varying $D$ with $\beta$ fixed equal to 0.293 | 0.293 (fixed) | $1.50 \pm 0.01$ |

Within the temperature region $0.003 < t < 0.03$, the theoretical prediction for the compressible Ising lattice is well approximated by a power law with an effective value of $\beta = 0.293$ and $D = 1.49$. Within this temperature region a least-squares fit of our data to a power law gives the results shown in Table II. It should be noted that there is a pronounced correlation of probable values of $\beta$ and $D$. This is seen by keeping one parameter, say $\beta$, fixed and allowing the other parameter to vary in the least-squares fit, as shown in the last row of Table II. Since we did not take much data close to $T_c$ and since the small size of our sample led to low intensities, we expect our value of $\beta$ to be less accurate than values obtained earlier.[3]

We conclude that there is excellent agreement between experimental data and the theoretical results for the compressible Ising lattice at all temperatures and this is clearly brought out in Fig. 2.

Finally, it should be noted that the experimental data on the order-disorder transition in $\beta$ brass[2-4] as a whole are in slightly better agreement with the compressible Ising lattice than with the rigid lattice – the final comparison will be published elsewhere.

## ACKNOWLEDGMENTS

We are indebted to G. A. Baker and J. W. Essam for allowing us to quote their results on the compressible Ising lattice prior to publication. Comments from M. E. Fisher are acknowledged, and we should like to thank J. Kjems for assistance in the experiments.

*Present address: Los Alamos Scientific Laboratory, Los Alamos, N.M. 87544.

†Present address: Brookhaven National Laboratory, Upton, N.Y. 11973.

[1] D. Chipman and B. E. Warren, J. Appl. Phys. 21, 696 (1950).

[2]O. W. Dietrich and J. Als-Nielsen, Phys. Rev. 153, 711 (1967).
[3]J. Als-Nielsen and O. W. Dietrich, Phys. Rev. 153, 717 (1967).
[4]J. Als-Nielsen, Phys. Rev. 185, 664 (1969).
[5]J. W. Essam and M. E. Fisher, J. Chem. Phys. 38, 802 (1967).
[6]J. W. Essam and D. L. Hunter, J. Phys. C 1, 392 (1968).
[7]J. W. Essam and G. A. Baker (private communications).
[8]C. Domb, J. Chem. Phys. 25, 783 (1956).
[9]E. A. Owen and L. Pickup, Proc. Roy. Soc. (London) A145, 258 (1934).
[10]D. N. Yoon and A. Bienenstock, Phys. Rev. 170, 631 (1968).
[11]W. C. Hamilton, Acta Cryst. 10, 629 (1957).
[12]J. M. Ziman, *Principles of the Theory of Solids* (Cambridge U. P., New York, 1964), Chap. 2.
[13]B. T. M. Willis, Acta Cryst. A25, 277 (1969).
[14]In determining the extinction correction at room temperature, the correction for lattice vibrations must be assessed. This correction was estimated using the Debye temperature given by D. Chipman [J. Appl. Phys. 31, 2012 (60)]. The extinction correction and lattice vibration corrections were then evaluated as described above and the latter were found to be close to the original estimates. These results were used in the evaluation of new values for the room-temperature extinction corrections and the values of $e^{-B(T)\hbar^2}$ were redetermined.

PHYSICAL REVIEW B VOLUME 2, NUMBER 2 15 JULY 1970

# Many-Electron Effects in the Optical Conductivity of Simple Metals by Kubo Formula*

A. O. E. Animalu

*Physics Department, University of Missouri, Rolla, Missouri* 65401

(Received 27 October 1969)

Starting from the Kubo formula for the optical conductivity, we review, reformulate, and generalize our previous one-electron theory of the optical absorption of solid and liquid alkali metals to include many-body effects due to electron-electron Coulomb interactions. The optical matrix element $\langle \psi_{k'} | \vec{\nabla} | \psi_k \rangle$, which was previously calculated in terms of an "optical pseudopotential," is rederived from a second-order scattering of an electron (quasiparticle in the many-body theory) by the Coulomb field of the ions and the applied photon field. The result is then represented by Feynman graphs similar in the lowest order to the "bremsstrahlung" of quantum electrodynamics, and shown, accordingly, to give rise to four categories of many-electron effects, viz., screening effects (usually incorporated in the one-electron approximation), electron self-energy effects, electron-photon and electron-ion vertex corrections, and final-state interactions. The changes of the one-electron result due to self-energy and to vertex corrections counteract each other in sodium and potassium, leading to no more than 10% net change; accordingly, the only appreciable enhancement comes from final-state interactions involving virtual exchange of plasmons, considered previously by Mahan.

## I. INTRODUCTION

In this paper we shall review, reformulate, and generalize our previous calculation[1,2] (hereafter referred to as AI and AII) of the optical conductivity $\sigma(\omega)$ of solid and liquid alkali metals, to include many-body effects due to electron-electron Coulomb interactions. In a subsequent paper, we shall consider a second aspect of many-body effects, namely, that due to *electron-photon-ion interaction* – its effects on the optical effective mass[3] and its implications on photon-induced superconductivity recently introduced by Kumar and Sinha.[4] The calculation to be reported in this paper will be based on the Kubo formula[5,6] and the optical pseudopotential method introduced in AI, since these approaches have been found to be both simple and in reasonable accord in the one-electron approximation with the recent measurements of the optical properties of sodium and potassium by Smith.[7] However, since many calculations of optical properties, both in the one-electron approximation[1,8] and including many-body effects,[9–18] exist in the literature, our emphasis will be on providing a simple and complete picture which will transcend all previous quantitative calculations, and furnish a basis for future investigations in this area. This simple picture – consisting essentially of a second-order scattering involving an electron-ion vertex and an electron-photon vertex similar to the "bremsstrahlung" of quantum electrodynamics – will be derived in Sec. IIB.